JLB

Article

Δ^9-Tetrahydrocannabinol-mediated epigenetic modifications elicit myeloid-derived suppressor cell activation via STAT3/S100A8

Jessica Margaret Sido, Xiaoming Yang,* Prakash S. Nagarkatti,* and Mitzi Nagarkatti*,†,1*

*Department of Pathology, Microbiology, and Immunology, University of South Carolina School of Medicine, Columbia, South Carolina, USA; and †WJB Dorn Veterans Affairs Medical Center, Columbia, South Carolina, USA

RECEIVED OCTOBER 10, 2014; REVISED JANUARY 8, 2015; ACCEPTED JANUARY 12, 2015. DOI: 10.1189/jlb.1A1014-479R

ABSTRACT

MDSCs are potent immunosuppressive cells that are induced during inflammatory responses, as well as by cancers, to evade the anti-tumor immunity. We recently demonstrated that marijuana cannabinoids are potent inducers of MDSCs. In the current study, we investigated the epigenetic mechanisms through which THC, an exogenous cannabinoid, induces MDSCs and compared such MDSCs with the naïve MDSCs found in BM of BL6 (WT) mice. Administration of THC into WT mice caused increased methylation at the promoter region of DNMT3a and DNMT3b in THC-induced MDSCs, which correlated with reduced expression of DNMT3a and DNMT3b. Furthermore, promoter region methylation was decreased at Arg1 and STAT3 in THC-induced MDSCs, and consequently, such MDSCs expressed higher levels of Arg1 and STAT3. In addition, THC-induced MDSCs secreted elevated levels of S100A8, a calcium-binding protein associated with accumulation of MDSCs in cancer models. Neutralization of S100A8 by use of anti-S100A8 (8H150) in vivo reduced the ability of THC to trigger MDSCs. Interestingly, the elevated S100A8 expression also promoted the suppressive function of MDSCs. Together, the current study demonstrates that THC mediates epigenetic changes to promote MDSC differentiation and function and that S100A8 plays a critical role in this process. *J. Leukoc. Biol.* 97: 677–688; 2015.

Introduction

MDSCs, which were originally observed in cancer models, are anti-inflammatory mediators that can be helpful or harmful depending on the context. In cancer models, MDSCs inhibit the T cell-driven response against tumors, allowing for cancer growth and metastasis [1, 2]. However, in autoimmune diseases, MDSC induction is advantageous, working to reduce proliferative T cell inflammation [3–6]. Therefore, it is necessary to understand the mechanisms that lead to MDSC induction and activation to use this duality best. MDSCs can be categorized in mice into 2 major subsets: granulocytic ($Ly6G^+Ly6C^+GR1^+CD11b^+$) or monocytic ($Ly6G^-Ly6C^+GR1^+CD11b^+$) [7]. Additionally, MDSCs are defined by their ability to suppress T cell responses, including proliferation [8, 9]. The classic mechanism for MDSC suppression of T cell proliferation is L-arginine metabolism via cytokine iNOS or NOS2 or Arg1 [10].

As gene regulation is integral for cell function and development, interest in dynamic epigenetic modifications has become paramount. DNA methylation, one of the most common forms of epigenetic regulation, controls gene expression by blocking transcription machinery, causing reversible gene silencing [11]. DNA methylation, de novo and inherited, is dependent on DNMTs [12], which transfer methyl groups from S-adenosyl-L-methionine to the 5-position on the cytosine residue found in CpG clusters within the DNA sequence [11]. DNMT1 binds preferentially to hemimethylated DNA and is considered to be the maintenance DNMT, and the DNMT3 family, 3a and 3b, is deemed necessary for de novo methylation [12]. Altered DNMT profiles are often seen in cancer patients, suggesting that global methylation is vital to proper cellular function, although no direct association between altered methylation profiles and MDSC induction has been highlighted in these studies [13, 14]. Furthermore, DNA methylation has been linked not only to immune function but also to immune cell differentiation [15–21]. Interestingly, MDSCs are not a terminally differentiated immune cell population. Rather, MDSCs are considered a heterogeneous mixture of immature myeloid-origin cells that can differentiate into DCs or macrophages [22]. It is the plasticity of

Abbreviations: AD = absolute density, Arg1 = arginase 1, BL6 = C57BL/6 mice, BM = bone marrow, CB = cannabinoid receptor, CEAS = Cis-regulatory Element Annotation System, CM = conditioned media, DC = dendritic cell, DNMT = DNA methyltransferase, HPC = hematopoietic progenitor cell, IDT = Integrated DNA Technologies, MDSC = myeloid-derived suppressor cell, MeDIP = methylated DNA immunoprecipitation,

(*continued on next page*)

The online version of this paper, found at www.jleukbio.org, includes supplemental information.

1. Correspondence: Dept. of Pathology, Microbiology, and Immunology, School of Medicine, University of South Carolina, 6439 Garners Ferry Rd., Columbia, SC 29209, USA. E-mail: mitzi.nagarkatti@uscmed.sc.edu

immature cells that suggests that DNA methylation could be playing a role in MDSC maintenance and activation. However, there is only 1 recent study indicating that histone deacetylase 11 may play a role as an epigenetic regulator in MDSC expansion and function [23].

THC, an exogenous cannabinoid derived from the *Cannabis sativa* plant, has long been known to act as an anti-inflammatory agent, as well as suppress the antitumor immune response [24–28]. The immunosuppressive properties of THC in cancer models were shown to be, in part, a result of the induction of Th2 anti-inflammatory cytokines (IL-4 and IL-10) and a correlating decrease of Th1 proinflammatory cytokines (IL-2 and IFN-γ) [24, 26]. THC has also been shown to induce T_{regs} [28, 29]. Additionally, recent studies from our laboratory have suggested that administration of THC into mice can trigger large numbers of immunosuppressive MDSCs [30].

Whereas it has been shown that THC can alter cytokines and transcription factors linked to MDSC differentiation or homing, its role in MDSC expansion and activation has not been clearly elucidated [30–32]. Furthermore, the role of epigenetic pathways in the induction of MDSCs by THC has not been determined. In the current study, we investigated the effect of THC on methylation of several genes involved in the differentiation and activation of MDSCs, and our data demonstrate epigenetic regulation of several of the critical molecules involved in MDSC activation and functions, including Arg1 and STAT3.

MATERIALS AND METHODS

Mice

Female BL6 (WT) mice, aged 6–8 weeks, at an average weight of 20 g, were obtained from the National Cancer Institute (Frederick, MD, USA). All mice were housed in pathogen-free conditions and allowed ad libitum access to filtered water and Teklad rodent Diet 8604 (normal chow) at the Animal Research Facility located at the University of South Carolina School of Medicine. All experiments were conducted under an approved Institutional Animal Care and Use Committee animal protocol.

Treatment with THC

THC (National Institute on Drug Abuse, NIH, Bethesda, MD, USA) dissolved in ethanol was diluted in 1× PBS to a concentration of 20 mg/kg. THC was administered i.p. into naïve mice. For depletion of S100A8, mice were given an i.p. injection of anti-S100A8 (0.01 mg/mouse 8H150), 1 h after THC treatment.

MDSC isolation

Sixteen hours after THC injection, mice were euthanized and the peritoneal exudate collected (3 washes of 5 ml ice-cold 1× PBS were injected into the peritoneal cavity and after 5 min, with agitation, collected). The cells were resuspended in 1 ml and then treated with Fc block for 10 min and labeled with PE-conjugated anti-Gr1 antibodies. The EasySep Mouse PE Positive Selection Kit procedure was followed to isolate Gr1-positive cells, as described [33]. After isolation, cells were labeled with FITC-conjugated anti-CD11b and assessed for purity by use of flow cytometric analysis gating on live cells. To isolate Ly6G- and Ly6C-positive cells, EasySep PE Positive and FITC Selection Kits were used, respectively. Purity of the MDSC subset populations was assessed by use of triple staining with Alexa Fluor 647-conjugated anti-CD11b.

mAb, reagents, and flow cytometer

Antibodies used for flow cytometric analysis (BioLegend, San Diego, CA, USA) include Fc block (93), PE-conjugated anti-Gr1 (RB6-8C5), FITC-conjugated anti-CD11b (M1/70), PE-conjugated anti-Ly6G (1A8), FITC-conjugated anti-Ly6C (HK1.4), and Alexa Fluor 647-conjugated anti-CD11b (ICRF44). In brief, peritoneal lavage cells (10^6 cells) from BL6 mice were incubated with FcR antibodies (5–10 min) and incubated with conjugated antibodies (20–30 min at 4°C). Next, cells were washed twice with 1× PBS/2% FBS buffer. The stained cells were then assessed by flow cytometer (FC500; Beckman Coulter, Brea, CA, USA) and the resulting data analyzed by Cytomics CXP software (Beckman Coulter). Two-color flow cytometric analysis was completed for assessing the presence of MDSCs in the BM and peritoneal exudates. Three-color flow cytometric analysis was used to profile the MDSC subsets.

MeDIP-seq

Purified genomic DNA was treated with dsDNA Shearase (Zymo Research, Irvine, CA, USA). DNA fragments with size from 200 to 400 bp were purified to construct sequencing library by use of the library ChIP-Seq Sample Preparation Kit (Illumina, San Diego, CA, USA). dsDNA was then denatured and immunoprecipitated with anti 5-methylcytosine antibody by use of a MeDIP Kit from Diagenode (Denville, NJ, USA). Precipitated DNA was purified and sequenced by HiSeq 2500 (Tufts Genomic Core, Boston, MA, USA). The sample before immunoprecipitation was also sequenced as input control.

MeDIP data analysis

MeDIP-seq libraries were sequenced with single-end reads of 50 bp. Raw sequencing reads were mapped to mouse genome build Mus musculus genome 9 (mm9) by use of Bowtie software by allowing 2 mismatches in the read [34]. The mapped reads were then filtered, and only uniquely mapped reads were used for the downstream analysis. Mapped reads were analyzed with MEDIPS software [35] and visualized in the Integrated Genome Browser (http://bioviz.org/igb). The location of 3 kb upstream and downstream of the TSS was generated by use of the University of California Santa Cruz table browser (UCSC Genome Bioinformatics; http://genome.ucsc.edu/). The DNA methylation signal of all genes within this region was extracted. The correlations of overall DNA methylation across the whole genome and near the TSS site (3 kb up- and downstream) were analyzed by CEAS software [36].

Msp PCR

Genomic DNA was isolated by use of the DNeasy Kit (Qiagen, Valencia, CA, USA), following the manufacturer's protocol. Bisulfite conversion of CpG islands was completed by use of the EpiTect Bisulfite Kit (Qiagen). Msp PCR was run with PreMix F (Epicentre, Madison, WI, USA) and iTaq DNA polymerase (BioRad Laboratories, Hercules, CA, USA). Samples were assessed for expression of DNMT3a (forward 5 CAGCACCATTCCTGGTCATGCAAA 3; reverse 5 TCAAGGTTTCCTGTCTGGTAGGCA 3) and DNMT3b (forward 5 GCACAACCAATGACTCTGCTGCTT 3; reverse 5 AGGACAAACAGC-GGTCTTCCAGAT 3) with an annealing temperature of 60°C. Additionally, methylated and unmethylated DNA primers were used for Arg1, NOS2, and STAT3 (**Table 1**). Methylation index {[(M)/(M + UM)] × 100}, where M is methylated, and UM is unmethylated, was used to assess DNA methylation. Universal Methylated Mouse DNA Standard (S8000; Millipore, Billerica, MA, USA) was used as a control with all primers. Primers were generated by use of Methyl Primer Express version 1.0 software and synthesized from IDT (Coralville, IA, USA).

(*continued from previous page*)

MeDIP-seq = methylated DNA immunoprecipitation sequencing service, mS100A8 = murine calgranulin A, Msp = methylation specific, P-STAT3 = phosphorylated STAT3, qPCR = quantitative PCR, RD = relative density, S100A8/9 = calgranulin A/B, THC = Δ^9-tetrahydrocannabinol, T_{reg} = T regulatory cell, TSS = transcription start site, WT = wild-type

TABLE 1. Primer sequences for the Msp PCR analysis of THC-induced and resident BM MDSCs

Gene	Primer	Sequence (5′–3′)	Annealing Temperature
Arg1	ARGMF	CGG GTT AAA TTC GGG TTA TC	55°C
	ARGMR	CGA ACT ACC GCG ATT CTA ATC	
	ARGUF	CCA AAC TAC CAC AAT TCT AAT CTA	
	ARGUR	TTT TGG GTT AAA TTT GGG TTA TT	
NOS2	NOS2MF	TAT ATA AAC GAG GTA TTC GCG C	55°C
	NOS2MR	CTT TAA CGC TAT CCC TTT ATC G	
	NOS2UF	GAA TAT ATA AAT GAG GTA TTT GTG T	
	NOS2UR	TCT TTA ACA CTA TCC CTT TAT CAC C	
STAT3	STATMF	GAG GTA TAA TTT TGT TTG GTG TT	60°C
	STATMR	AAA CCC AAC TAA CCA ACC TA	
	STATUF	GGT ATA ATT TCG TTC GGT GTC	
	STATUR	AAC CCG ACT AAC CGA CCT	

Effect of MDSCs on T cell proliferation

To study the ability of MDSCs to suppress T cell proliferation, we used the following assay as described [32]. Con A-activated (2.5 μg/ml) spleen cells from naïve BL6 mice were cultured in triplicate (0.2 ml/well in a round-bottom, 96-well plate) with mitomycin C-inactivated MDSCs for 38–40 h. The ratio of MDSCs:T cells was 1:25 (see Fig. 1B only) or 1:2. Sixteen hours before collection and analysis, [^{3}H]thymidine (2 μCi/well) was added to the cell cultures. [^{3}H]Thymidine incorporation was measured by use of a liquid scintillation counter (MicroBeta TriLux).

Western blot analysis

Protein was isolated from purified MDSCs by use of radioimmunoprecipitation lysis buffer (Santa Cruz Biotechnology, Santa Cruz, CA, USA), as described [37]. Five or 10 μg protein was loaded and ran on a polyacrylamide gel (12%) at 60 V for 2.5 h. Protein was then transferred to nitrocellulose at 100 V for 1 h. Protein transfer was confirmed by use of 3 ml Ponceau S staining solution. Nitrocellulose was then blocked in 5% nonfat dry milk in TBS. Nitrocellulose was then probed with antibodies to S100A8 (M-19 1:2000), S100A9 (M-19 1:1000), Arg1 (V-20 1:1000), NOS2 (iNOS; M-19 1:500), STAT3 (C-20 1:200), and P-STAT (9E12 1:200). HRP-conjugated secondary antibodies were used at 1:1000 or 1:2000 dilutions depending on the secondary required. For control protein bands, γ-tubulin (Poly6209) or β-actin (Poly6221) was used at a dilution of 1:1000. ECL substrate (Thermo Scientific, Rockford, IL, USA) was added for 1 min; exposure time varied.

ImageJ

Densitometry was performed on scanned Western blot images, as well as PCR gels, by use of the ImageJ gel analysis tool [38]. Scanned blots and gels were assessed for AD, as determined by the area under the curve of each experimental and control band. RD for Western blots was determined by dividing the experimental band AD by the control band AD for the protein of interest and a structural protein. The normalized density ratio was then calculated by dividing the protein of interest RD by the structural protein RD.

Cytokine analysis in cell culture supernatants

ELISA MAX sandwich ELISA kits (BioLegend, San Diego, CA, USA) were used to assess the level of IL-6, IL-10, and IFN-γ cytokines. Sandwich ELISA kits (MyBioSource, San Diego, CA, USA) were used to assess S100A8 and S100A9 levels. Isolated MDSCs from the BM or peritoneal cavity (2.5×10^6 cells/ml) from naïve or THC-treated mice were cultured in 0.2 ml aliquots in 96-well, round-bottom, tissue-culture plates for 16–20 h. Cytokine production was quantified from cell supernatants (stored at −20°C). Absorbance was measured at 450 nm by use of a VICTOR2 1420 MultiLable Counter (Wallac; PerkinElmer, Waltham, MA, USA).

qPCR

Total RNA was isolated and purified by use of the miRNeasy Kit (Qiagen), following the manufacturer's procedure. The iScript cDNA Synthesis Kit (BioRad Laboratories) was used, according to the manufacturer's specifications to reverse transcribe cDNA. qPCR was performed by use of SsoAdvanced SYBR Green (BioRad Laboratories) on a CFX Connect (BioRad Laboratories). Samples were assessed for expression of β−actin (forward 5 GGCTGTATTCCCCTCCATCG 3; reverse 5 CCAGTTGGTAACAATGCCATGT 3), IL-6 (forward 5 CAACGATGATGCACTTGCAGA 3; reverse 5 GGTACTCCAGAAGACCAGAGG 3), and IL-10 (forward 5 GCTCTTACTGACTGGCATGAG 3; reverse 5 CGCAGCTCTAGGAGCATGTG 3). Primers were synthesized from IDT with annealing temperatures of 60°C.

Cell culture with CM or recombinant S100A8 protein

Isolated MDSCs were plated with Con A-activated splenocytes at a ratio of 1:2 (MDSC:Con A splenocytes). CM were made by incubating isolated THC-induced MDSCs with PMA and calcium ionophore ionomycin (50 ng/ml and 10 μg/ml, respectively) for 5 h. Lyophilized S100A8 protein (mS100A8; MyBioSource) was reconstituted in complete RPMI media (1% vol/vol penicillin/streptomycin, 1% vol/vol HEPES buffer, 10% vol/vol heat-inactivated FBS, and 0.0002% vol/vol 2-ME). mS100A8 (2000 ng) was added at 0 and 24 h to cell-culture wells.

Statistical analysis

Data are shown as mean ± SEM. Student's *t*-test was used to compare data between 2 groups. One-way ANOVA with Tukey post hoc test was used to compare 3 or more groups. Experimental groups were compared with controls; $P < 0.05$ was considered significant.

RESULTS

T cell suppression is increased in THC-induced MDSCs

The largest accumulation of resident MDSCs is located in the BM [10]. It has been shown that MDSCs migrate from this repository to sites of inflammation by following chemokine/

cytokine signals [10]. Our lab has shown that MDSCs will also migrate to the peritoneal cavity after a single THC injection (i.p.) [30]. With the knowledge that the peripheral MDSCs are considered active and therefore, T cell suppressive, we first determined if any differences existed between the resident BM MDSCs and the THC-induced MDSCs found in the peritoneal cavity. As such, naive BL6 (WT) mice were given a single i.p. injection of THC to cause massive induction of MDSC to the peritoneal cavity, as described earlier [30]. Sixteen hours after THC treatment, peritoneal lavage was used to collect peripheral THC-induced MDSCs. Resident BM MDSCs from naïve BL6 mice were used as controls. MDSCs were purified (>95%) by use of positive-selection magnetic beads. Flow cytometry was used to determine if any differences in MDSC and MDSC subset populations existed. The naïve BM showed ~51% of $Gr1^+CD11b^+$ cells when compared with THC-induced peritoneal cells that contained ~83% $Gr1^+CD11b^+$ cells (**Fig. 1A**). Next, we sorted the $Gr1^+CD11b^+$ cells and stained them further for Ly6G and Ly6C to measure granulocytic ($Ly6G^+Ly6C^+Gr1^+CD11b^+$) and monocytic ($Ly6G^-Ly6C^+Gr1^+CD11b$) MDSC subset proportions (Fig. 1D). To demonstrate that the THC-induced $Gr1^+CD11b^+$ cells were, in fact, T cell suppressive, we tested the levels of IFN-γ secretion, which decrease significantly upon addition of THC-induced MDSCs to activated T cells (Fig. 1B). We next assessed the suppressive capabilities of THC-induced MDSCs compared with resident BM MDSCs. We found that THC-induced MDSCs were significantly more suppressive of Con A-activated, splenic T cells than the resident BM MDSCs (Fig. 1C). With literature suggesting that MDSC subsets can have differing levels of suppression, we compared independently isolated $Gr1^+$, $Ly6G^+$, or $Ly6C^+$ MDSC subsets; $Ly6C^+$ subsets were isolated after positive selection of $Ly6G^+$ cells by use of concurrent PE- and FITC-positive selection for Ly6G and Ly6C, respectively [39, 40]. The individually isolated, pure MDSC subpopulations were then treated with mitomycin C and added to Con A-activated spleen cells at an MDSC:spleen cell ratio of 1:2 to study the ability of MDSCs to inhibit T cell proliferation (Fig. 1E). In all 3

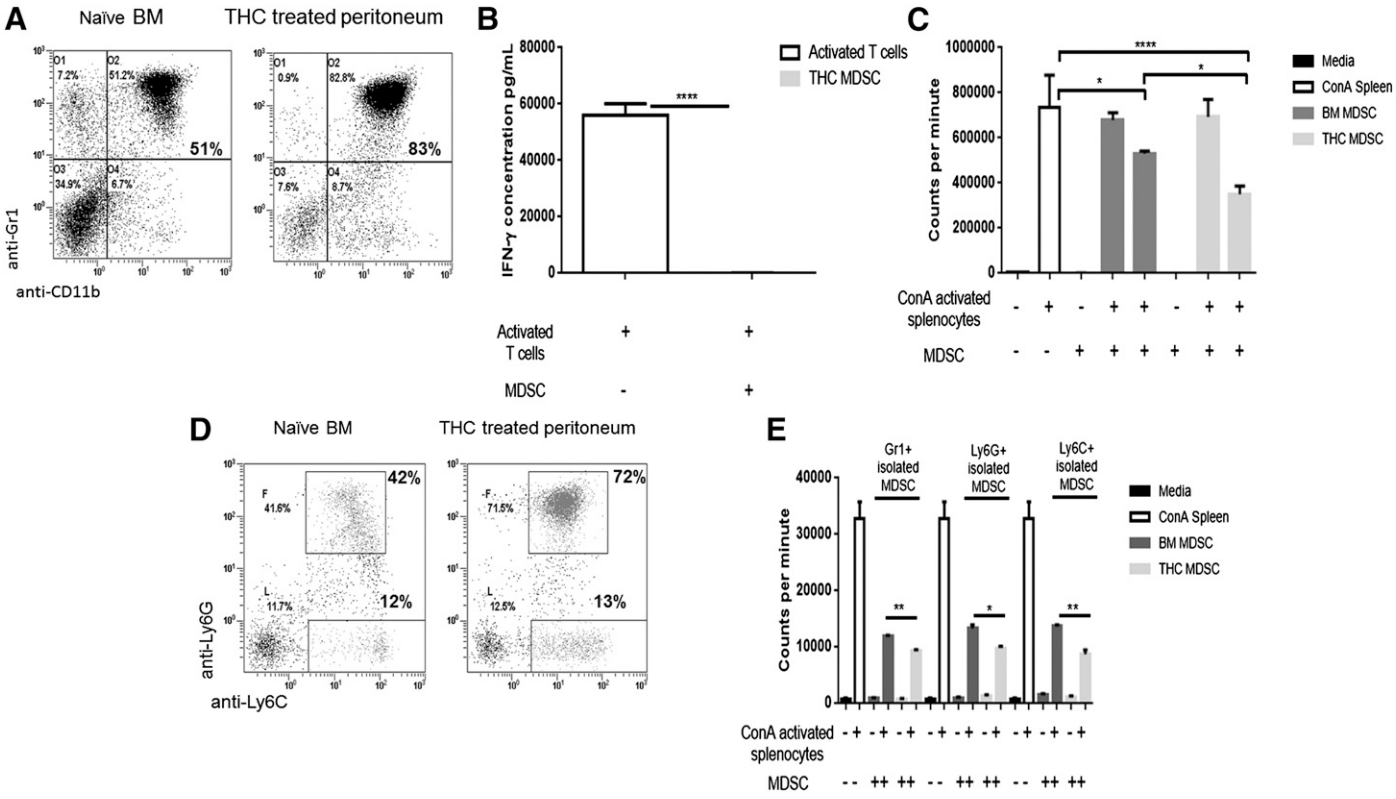

Figure 1. THC-induced MDSCS differ from resident BM MDSCs in subset proportion and suppressive functionality. MDSCs were isolated from peritoneal exudates at 16 h after THC injection, and naïve BM with the use of positive selection magnetic beads for αGr1, αLy6G, or αLy6C. MDSCs were mitomycin C treated before plating with BL6 spleen cells activated with Con A (MDSC:T cell ratios 1:25 and 1:2). IFN-γ was assessed in cell supernatants by use of sandwich ELISA kits (BioLegend) after coculture. Proliferation of spleen cells was assessed 40 h after stimulation by use of [^{3}H]thymidine (cocultured for 16 h). (A) Flow cytometric analysis for MDSC proportion (dot plots gated only on live cells), double-stained for $GR1^+CD11b^+$ cells in naïve BM (left) and THC-treated peritoneal exudate (right). (B) Levels of IFN-γ secreted by activated T cells, with and without MDSC coculture. (C) Ability of MDSCs to suppress proliferation of T cells. MDSCs from naïve BM or THC-treated peritoneal exudate MDSCs were cocultured with Con A-activated splenic T cells. (D) Flow cytometric analysis of MDSCs from naïve BM (left) or THC-treated peritoneal exudate (right) MDSCs following triple-staining with $CD11b^+$, $Ly6G^+$, and $Ly6C^+$ cells (dot plots gated on CD11b-positive cells). (E) Suppression of T cell proliferation by $Gr1^+$, $Ly6G^+$, and $Ly6C^+$ cells isolated from naïve BM and THC-treated peritoneal exudate cocultured with Con A-activated splenic T cells. Representative data from replicate experiments (mean ± SEM); $*P < 0.05$, $**P < 0.01$, $****P < 0.0001$, ANOVA/Tukey.

isolation conditions—Gr1$^+$, Ly6G$^+$, or Ly6C$^+$—THC-induced MDSCs showed significantly more suppression of T cell proliferation than resident BM MDSCs (Fig. 1E).

THC-induced MDSCs exhibit differential expression of functional proteins

To explain how THC-induced MDSCs exhibited increased suppressive capabilities compared with resident BM MDSCs, we next looked at the expression of functional proteins. The ability of MDSC to suppress T cell proliferation has been linked to elevated expression of L-arginine metabolizers Arg1 or NOS2 [41]. The expression of Arg1 was increased greatly in THC-induced MDSCs compared with resident BM MDSCs (**Fig. 2A**). To ensure that Arg1 expression was specific to activated MDSCs, we looked at BM and splenic MDSCs from naïve mice, as well as BM, splenic, and peritoneal MDSCs from THC-treated mice. We found no expression of Arg1 in naïve or BM resident MDSCs, although peripheral MDSCs in THC-treated mice did exhibit Arg1 expression (Supplemental Fig. 1A). However, NOS2 expression was reduced in THC-induced MDSCs isolated from the peritoneal cavity compared with naïve resident BM MDSCs (Fig. 2B). We also looked at the expression of the S100A8 and S100A9 proteins, as a result of the fact that although cancer studies have determined that secretion of S100A8 and S100A9 is associated with tumor-induced MDSCs, no one has linked THC-mediated induction of MDSCs to the expression of these S100 proteins [42]. Elevated levels of S100A8, but not S100A9, were observed in THC-induced MDSCs when compared with BM MDSCs (Fig. 2C and D, respectively). As STAT3 plays a critical role in MDSC expansion, activation, and function, we investigated the expression of P-STAT3 [43–45]. Interestingly, THC-induced MDSCs showed an increased expression of P-STAT3/STAT3 when compared with resident BM MDSCs (Fig. 2E).

STAT3-associated cytokines are up-regulated in THC-induced MDSCs

It has been shown recently that Arg1 and S100A8 are downstream targets of STAT3 [31, 46, 47]. As such, we looked at the spontaneous secretion of IL-10 and IL-6, known STAT3-activating cytokines, from MDSCs cultured overnight after isolation. Spontaneous secretion of IL-10 was low from both MDSC populations. However, THC-induced MDSCs secreted significantly more IL-10 than did resident BM MDSCs (**Fig. 3A**). This correlated with elevated expression of the IL-10 message in THC-induced MDSCs (Fig. 3C). Spontaneous IL-6 secretion, as well as the transcript, was expressed at higher levels in THC-induced MDSCs when compared with resident BM MDSCs (Fig. 3B). This trend was supported by a significantly increased IL-6 message in THC-induced MDSCs (Fig. 3D).

THC treatment increases S100A8 secretion

As STAT3 can regulate S100 proteins [47], we next determined the levels of S100A8 and S100A9. THC-induced MDSCs showed significantly increased S100A8, but not S100A9, secretion when compared with resident BM MDSCs (Fig. 3E and F, respectively). Furthermore, we found that injection of THC systemically increased S100A8 levels compared with naïve mice (Fig. 3G).

THC administration alters the methylation profile in MDSCs as a result of decreased DNMTs

We next determined whether THC induces MDSCs through epigenetic regulation. To that end, we first determined if THC could affect methylation by studying global changes in genomic DNA methylation patterns. We found that whereas overall methylation was unaffected by THC treatment, with the use of CEAS software for correlational analysis, the methylation at promoter regions was altered when resident BM and THC-induced MDSCs were compared (**Fig. 4A** and **B**, respectively). Knowing that methylation changes could occur as

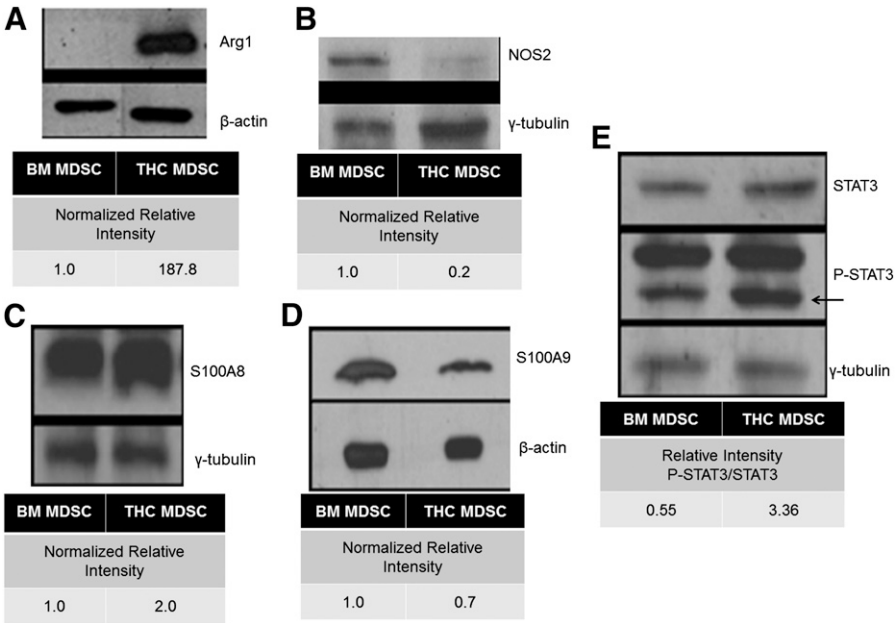

Figure 2. THC-induced MDSCs have differential expression of MDSC-associated proteins compared with resident naïve BM MDSCs. Western blot, followed by densitometric analysis via ImageJ with β-actin or γ-tubulin used for normalization. MDSC-associated proteins, including, (A) Arg1, (B) NOS2, (C) S100A8, (D) S100A9, and (E) STAT3 (P-STAT3), in MDSCs derived from naïve resident BM and THC-induced peritoneal exudate. Representative data from triplicate experiments (mean ± SEM).

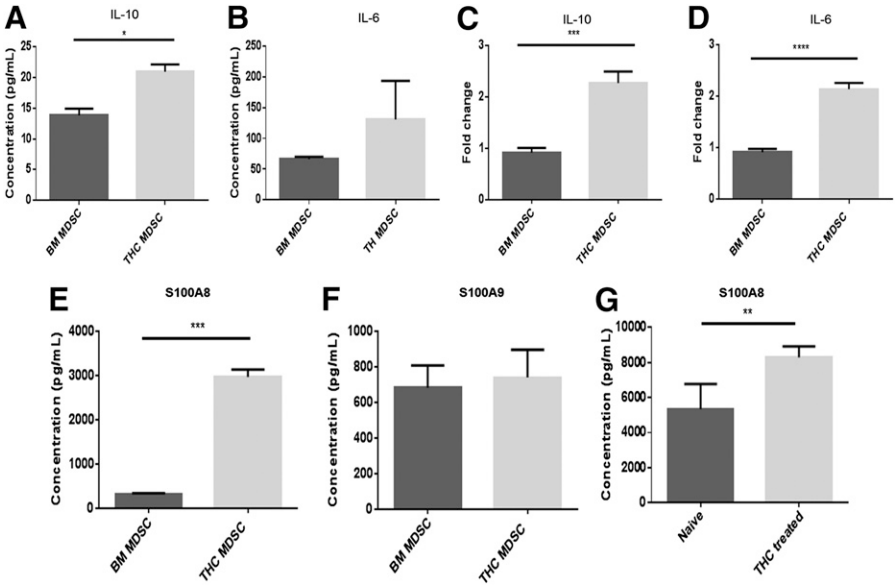

Figure 3. THC-induced MDSCs exhibit elevated levels of cytokines associated with STAT3 activation. THC-induced MDSCs and resident naïve BM MDSCs were cultured overnight and cell supernatants collected for cytokine analysis by use of sandwich ELISA kits: (A) IL-10 and (B) IL-6. cDNA was isolated from MDSCs for real-time qPCR analysis: (C) IL-10 mRNA and (D) IL-6 mRNA. Spontaneous secretion from THC-induced and resident naïve BM MDSC culture supernatants: (E) S100A8 and (F) S100A9. Serum from THC-treated or naïve mice was analyzed for S100: (G) S100A8 levels. Representative data from replicate experiments (mean ± SEM); $*P < 0.05$, $**P < 0.01$, $***P < 0.005$, $****P < 0.0001$, Student's *t*-test.

a result of differential expression of DNMTs, specifically, DNMT3a and DNMT3b, which are responsible for de novo methylation, both resident BM and THC-induced MDSCs were assessed for DNMT methylation and mRNA expression [48, 49]. The methylation at the promoter region for DNMT3a and DNMT3b was increased in THC-induced MDSCs (Fig. 4C). Additionally, THC-induced MDSCs had significantly reduced expression of DNMT3a and DNMT3b compared with resident BM MDSCs (Fig. 4D).

THC decreases the methylation of key MDSC functional genes

We next investigated if the changes in Arg1, NOS2, and STAT3 seen in THC-induced MDSCs resulted from alterations in the methylation of these key genes associated with MDSC activation and function. With the use of Methyl Primer Express version 1.0 software, individual gene methylation primers were developed for key genes associated with the suppressive function of MDSCs (Table 1). Furthermore, universally methylated mouse DNA (Universal Methylated Mouse DNA Standard; Millipore) was used as a baseline for comparisons between resident BM and THC-induced MDSC methylation. With the use of CEAS software, we observed that promoter region methylation was decreased at Arg1 and STAT3 in THC-induced MDSCs (**Fig. 5A** and **B**, respectively). To support the findings from the genomic DNA methylation analysis, we used Msp PCR. The methylation index showed that THC-induced MDSCs had deceased levels of methylation at Arg1 and STAT3, but not at iNOS, compared with naïve resident BM MDSCs (Fig 5C). Methylation of S100A8 and S100A9 proteins was not determined, as there were no CpG islands found in the promoter regions of these genes. Together, these data demonstrated that THC induces immunosuppressive MDSCs through hypomethylation of critical genes that regulate MDSC functions.

S100A8 is important in maintaining a suppressive, peripheral MDSC population

To elucidate further the role that S100A8 was playing in MDSC functionality, we first created a CM, which contained both STAT3-activating cytokines that could enhance Arg1 production and soluble S100A8. CM was created by incubating THC-induced MDSCs in the presence of PMA (50 ng/ml) and calcium ionophore (10 μg/ml). Resident BM MDSCs were then plated with or without CM and Con A-activated splenocytes. Resident BM MDSCs caused just >25% suppression of T cell proliferation in response to Con A compared with THC-induced MDSCs that caused 50% suppression (**Fig. 6A**). However, resident BM MDSCs in CM had significantly increased suppressive capabilities, reducing T cell proliferation by nearly 70%, compared with BM MDSCs without CM (Fig. 6A).

To determine further the role of S100A8 in vivo, we treated THC-injected mice with a single dose of S100A8 antibody (8H150). The mice were then assessed for MDSC induction in the peritoneal cavity for >16 h via flow cytometric analysis of $Gr1^+CD11b^+$ cells. The S100A8 antibody caused a significant decrease in MDSC accumulation in the peritoneal cavity at the 16 h time-point (Fig. 6B). Furthermore, looking at MDSC subsets, we found that upon blocking S100A8, significantly fewer granulocytic MDSCs were induced by THC, whereas no significant reduction was seen in monocytic MDSCs (Fig. 6C and D, respectively). Additionally, to ascertain the role of S100A8 in MDSC-induced suppression of T cell proliferation, recombinant protein (mS100A8) was added to plated resident BM MDSCs in the presence of Con A-activated splenocytes. A significant increase in suppression was seen in resident BM MDSCs treated in vitro with mS100A8 compared with untreated resident BM MDSCs (Fig. 6E). Furthermore, mS100A8-treated resident BM MDSCs were able to suppress T cell proliferation to a similar level as THC-induced MDSCs (Fig. 6E).

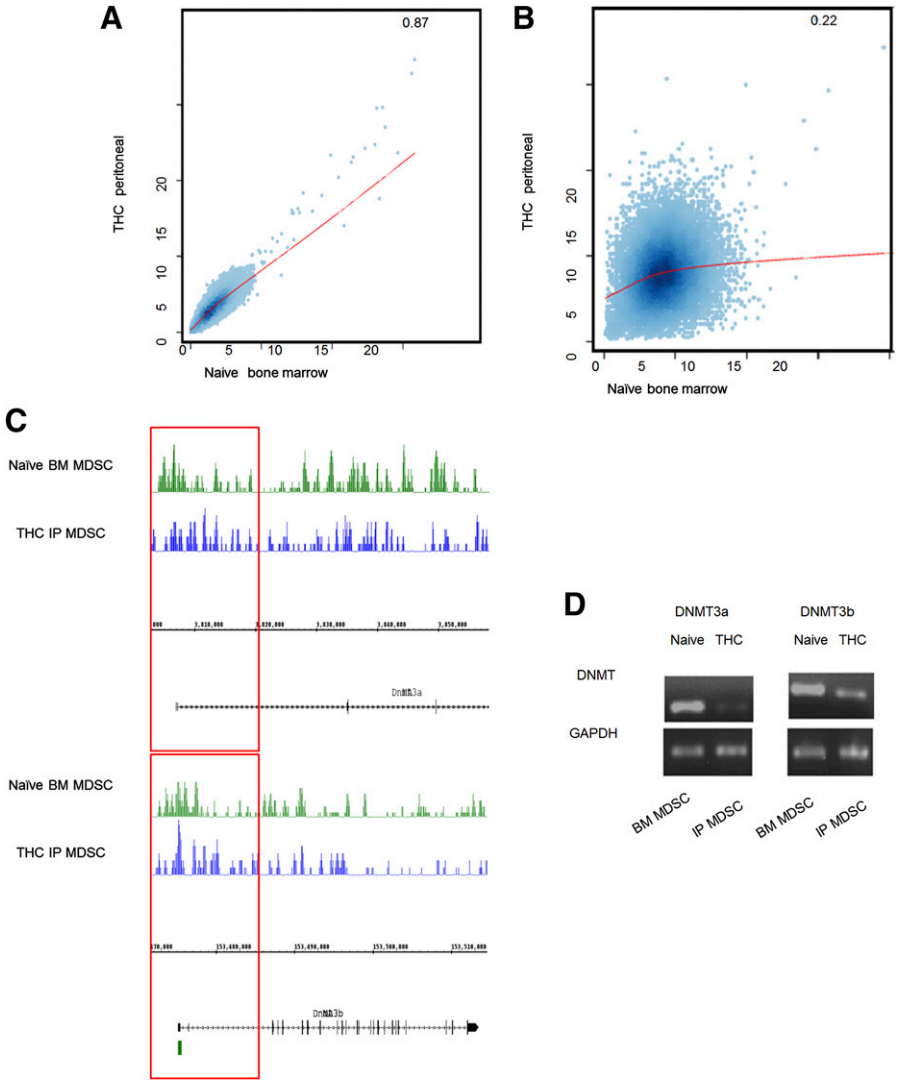

Figure 4. THC alters the methylation profile of MDSCs. Genomic DNA from THC-induced MDSCs (n=5 mice) and naïve resident BM MDSCs (n=5 mice) was assessed for genomic methylation via MeDIP-seq. (A) Correlations of genome-wide DNA methylation signal (CEAS software) in THC-induced and resident BM MDSCs. (B) Correlations of DNA methylation within 3 kb up- and downstream of the TSS in THC-induced and resident BM MDSCs. (C) DNA methylation near the TSS of DNMT3a and -3B (upper and lower, respectively). IP, i.p. (D) PCR for DNMT3a and -3b message in THC-induced and resident BM MDSCs. Representative data from replicate experiments.

DISCUSSION

The mechanisms through which THC mediates immunosuppression include apoptosis, induction of T_{regs}, and the induction of a switch from Th1 to Th2 phenotype [25, 26, 50]. Recently, our laboratory made an exciting finding that THC can induce massive numbers of MDSCs in vivo via activation of accessory immune cells, such as mast cells [30, 32]. MDSCs are a heterogeneous and immature cell population with an innate plasticity. Recently, studies have highlighted this plasticity by showing that MDSC subsets can induce TH17 or T_{regs} [51]. It has also been found that MDSCs, which are generally considered beneficial in the tumor microenvironment, secrete soluble factors, such as NO, which can induce apoptosis in cancer cells [52]. Together, these findings highlight the need to understand what factors are associated with MDSC plasticity, and it is likely that epigenetic modulation may be one of the contributing factors. As such, the focus of the current study was to elucidate further the mechanisms through which THC induces and maintains a peripheral population of highly immunosuppressive MDSCs. Recently, it has been shown that THC treatment can alter gene specific methylation patterns in lymphocytes [53]. Consequently, we set out to determine the role of altered DNA methylation in the context of THC-driven recruitment of MDSCs.

Research showing the involvement of THC in epigenetic modifications is limited. However, there is evidence suggesting that THC, ingested through marijuana abuse, can elicit indirect and direct effects on gene expression [31, 54–58]. Additionally, studies that use SIV-infected animals treated with THC found that up to 50% of all gene expression alterations were a result of differential DNA methylation patterns [59]. Furthermore, a CB1-dependent link with cannabinoid treatment was discovered in the regulation of keratinocyte differentiation by inducing DNA methylation [60]. Such findings support the role of CB1 receptor agonists, such as THC, in altering DNMT activity, resulting in changes in genomic DNA methylation patterns, as seen in the current study.

Alteration of DNMT expression correlates directly with changes to a gene loci-specific DNA methylation pattern [61]. Specifically, the changes in the methylation profile for

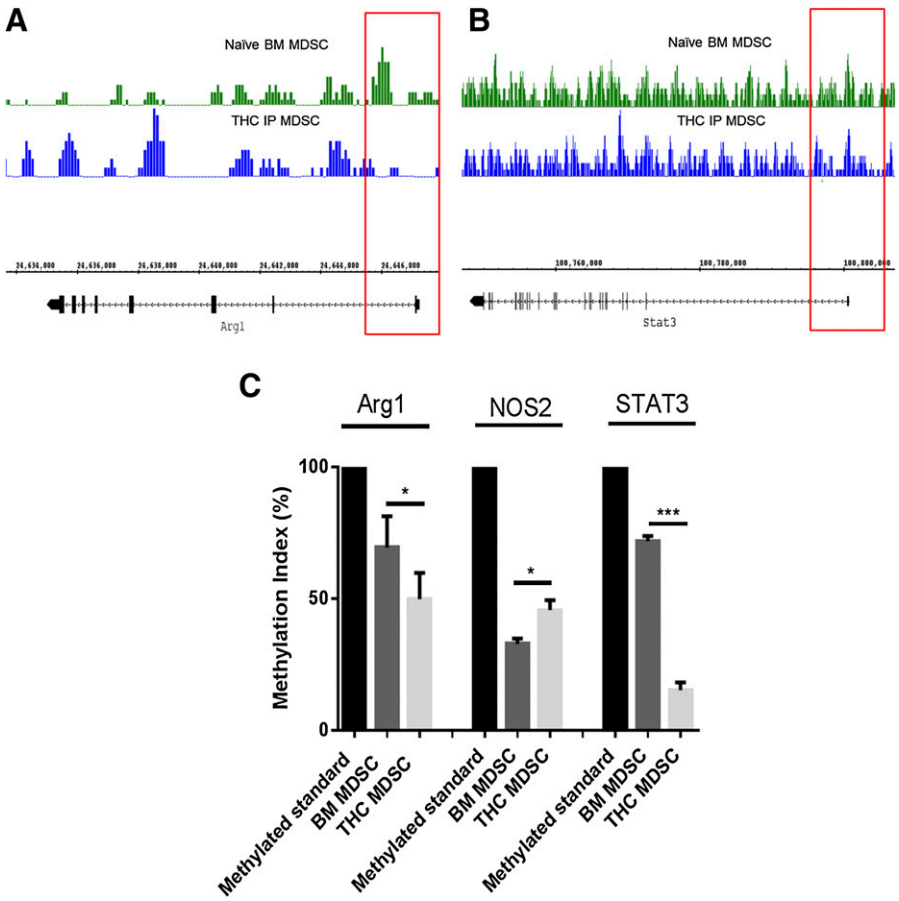

Figure 5. THC-induced MDSCs differ from resident BM MDSCs in promoter region methylation. Bisulfite-converted genomic DNA was assessed for promoter region-associated methylation in THC-induced and naïve BM MDSCs. (A) DNA methylation near the TSS of Arg1 in THC-induced and resident BM MDSCs. (B) DNA methylation near the TSS of Stat3 in THC-induced and resident BM MDSCs. Msp PCR products were run on agarose gel (2%) and densitometry assessed by use of ImageJ. (C) Methylation index for Arg1, NOS2, and STAT3 in THC-induced and resident BM MDSCs (fully methylated mouse DNA was used as a control). Data from replicate experiments (mean ± SEM); $*P < 0.05$, $***P < 0.005$, Student's *t*-test.

transcription factors associated with MDSC activation or function, such as STAT3, were of paramount interest to us, as elevated expression of STAT3 has been tied to increased MDSC-mediated immunosuppression [31, 43, 44, 62]. We found that STAT3 levels were increased significantly in THC-induced MDSCs. It has been shown that STAT3 activation, via IL-6 or G-CSF, is necessary for the expansion of functional MDSCs, in part, as a result of regulation of NADH oxidase [63]. Consistent with this, we also noted a significant increase in IL-6 in THC-induced MDSCs. Additionally, it has been shown that the highly suppressive nature of activated MDSCs, via Arg1 expression, is STAT3 dependent [45]. With STAT3 playing such an integral role in MDSC functionality, the differential expression that we observed between resident BM and THC-induced MDSCs suggested that resident MDSCs may exist in a naïve or inactivated state.

One of the hallmarks of MDSC function is their ability to suppress T cell proliferation. MDSCs have been shown to inhibit T cell activation and proliferation via L-arginine metabolism, oxidative stress, T_{reg} expansion, and cysteine depletion [64–68]. Previously, we showed that THC-induced MDSCs have elevated levels of Arg1 expression, thereby causing the suppression of T cell proliferation through L-arginine depletion [30]. In the current study, we also noted that THC-induced MDSCs had higher levels of Arg1 when compared with resident BM MDSCs. Furthermore, THC treatment has been associated with, a CB-dependent, loss of NOS2 activation as a result of cAMP signal inhibition [69, 70]. This may explain why in the current study, THC-induced MDSC did not exhibit an increase in NOS2. Additionally, the S100 proteins, S100A8 and S100A9, have been linked to MDSC expansion via the receptor for advanced glycation endproducts in cancer models [42]. In conjunction with reported findings, the elevated expression of Arg1 and S100A8 that we observed in the current study strengthens our claim that a single THC injection generates primed or activated, peripheral MDSCs rather than just recruiting inactivated BM MDSCs to the periphery.

Although S100A8/A9 has been associated with MAPK and NF-κB signaling pathways, these S100 proteins can also be linked to the JAK/STAT pathway [71]. For instance, S100A8 has been associated with STAT3-activating cytokines, including IL-10, in alveolar macrophages and IL-6 induction in PBMCs, creating an indirect association with the JAK/STAT signal pathway that we also observed in MDSCs [72, 73]. More directly, P-STAT3 is known to have binding sites in the promoter region of S100A8 [47]. This positive-feedback interaction between STAT3 and S100A8 suggests that the S100 protein may play a vital role in MDSC function.

HPCs maintain detectable levels of S100A8, for up to 1 week in culture, even upon differentiation, at which point, S100A9 expression is lost [47]. The role that S100A8 plays in MDSC function, however, has not been reported. It has been shown that

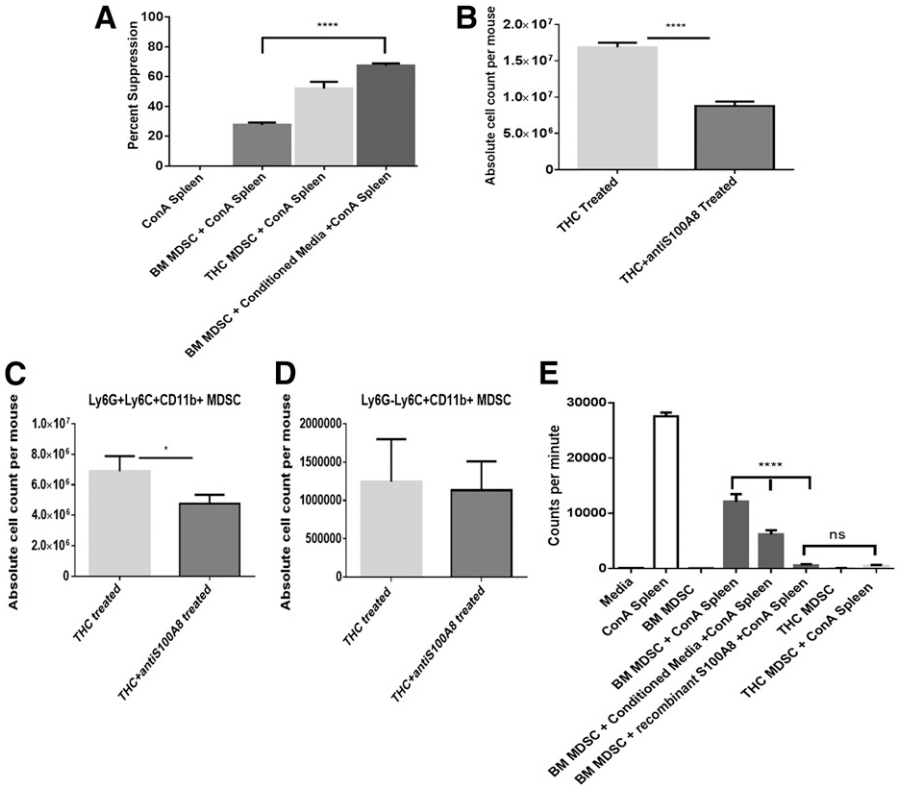

Figure 6. S100A8 protein impacts MDSC induction and activation. CM was obtained from THC-induced MDSCs, cultured for 5 h in the presence of PMA and calcium ionophore, and then assessed for suppressive capabilities. (A) The ability of CM to enhance MDSCs. Thymidine incorporation was used to detect T cell proliferation, and percent suppression, when compared with controls, was plotted. (B–D) Effect of anti-S100A8 antibodies on THC-induced MDSCs in the peritoneal cavity. Antibody (8H150) against S100A8 was administered 1 h after THC treatment and assessed for MDSC accumulation. Data indicate absolute cell counts of (B) $Gr1^+CD11b^+$, (C) granulocytic MDSCs ($Ly6G^+LyC^+CD11b^+$), and (D) monocytic MDSCs ($Ly6G^-Ly6C^+CD11b^+$) cells in the peritoneal cavity. (E) Effect of addition of recombinant S100A8 protein (mS100A8) on the ability of MDSCs to suppress T cell proliferation, which was studied by activation via use of Con A, as described above. The cultures received CM or mS100A8, as indicated. Representative data from replicate experiments (mean ± SEM); $^*P < 0.05$, $^{****}P < 0.0001$, Student's *t*-test or ANOVA/Tukey.

S100A8 is involved in granulocyte chemotaxis and that S100A8/A9 secretion allows for MDSC accumulation [42, 74]. A study by Hiroshima et al. [72] observed a correlation between elevated S100A8 and Arg1 transcript levels in alveolar macrophages. This finding supports our claim that increased S100A8 expression impacts MDSC function as an anti-inflammatory molecule similar to IL-10 [72, 75–77]. TLR activation can also be influenced positively by the S100A8 protein [78]. The current study, to the best of our knowledge, is the first one to report that elevated S100A8 levels in MDSCs regulate increased Arg1-driven T cell suppression.

A connection between increased S100A9 expression and the accumulation of tumor-associated MDSCs has been reported [47]. Cheng et al. [47] determined that CT-26, a tumor-cell CM, was able to increase S100A9 expression in vitro in HPCs, which correlated with a loss of DC differentiation. Additionally, Cheng et al. [47] were able to show that the MDSCs, accumulated via S100A9 overexpression, were, in fact, T cell suppressive. Although inflammation has been shown to induce MDSC recruitment, THC treatment recruits active MDSCs without proinflammatory signals [30]. Moreover, our studies showed that S100A9 was not induced by THC.

The ability of THC to alter gene expression via the up-regulation of key microRNA has also been studied. A single THC treatment was found to induce miR-690 overexpression in conjunction with decreased C/EBPα, a transcription factor associated with myeloid cell differentiation, in peripheral MDSCs [31]. Specifically, over expression of C/EBPα, alone, was sufficient to increase the expression of the S100A9 protein, which is known to decrease in mature differentiated cells [79]. As such, it has been suggested that the attenuation of C/EBPα could play a role in maintaining an immature, and therefore, functional, population of MDSCs upon THC induction [31].

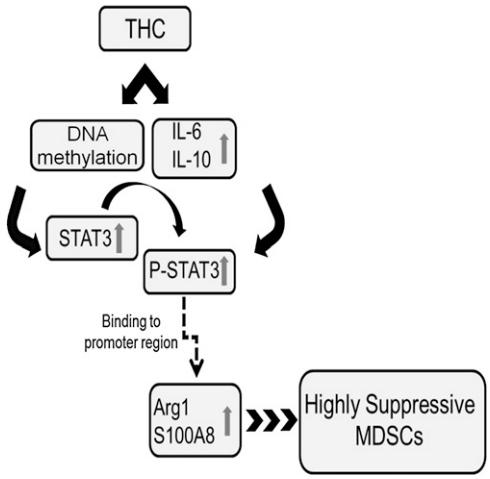

Figure 7. Proposed working model for the mechanism of MDSC induction and activation by THC. THC treatment causes hypomethylation of genes associated with MDSC function, such as STAT3, allowing for reduced gene silencing. Additionally, THC treatment increases the STAT3-activating cytokines IL-6 and IL-10. P-STAT3 is then able to bind the promoter region of S100A8 and Arg1, increasing the suppressive capability of the THC-induced MDSCs.

THC, causing a reduction of C/EBPα levels, and therefore, decreasing S100A9 expression, strengthens our claim that a S100A8-driven mechanism for THC-induced MDSC activation plays a critical role.

The mechanism of MDSC activation is one that remains elusive as a result of the variety of environmental factors that are known to impact the generation, maintenance, and function of these regulatory cells. The current study attempted to highlight a mechanism by which THC caused the induction and activation of primed peripheral MDSCs, depicted in **Fig. 7**. After THC treatment, there is decreased methylation of STAT3, leading to an up-regulation of the transcription factor, as well as STAT3-activating cytokines (IL-10 and IL-6), which together, lead to increased P-STAT3. Whereas low levels of IL-10 were secreted by THC-induced MDSCs, the ability of THC to activate additional IL-10-secreting cells, such as T_{regs}, further supports that THC plays a role in STAT3 activation [80]. P-STAT3 binds to the promoter region of S100A8 and Arg1, thereby increasing the expression of these proteins. Additionally, upon overexpression of S100A8 and Arg1, MDSCs became highly immunosuppressive. To the best of our knowledge, this report is the first one to identify a gene-specific methylation profile of MDSCs following THC treatment and how such epigenetic changes regulate the anti-inflammatory properties of MDSCs involving a STAT3/S100A8 positive-feedback loop.

AUTHORSHIP

P.S.N., M.N., and J.M.S. provided the experimental design and the manuscript evaluation. J.M.S. and X.Y. performed experiments and analysis. P.S.N., M.N., J.M.S., and X.Y. interpreted data. J.M.S. wrote the manuscript.

ACKNOWLEDGMENTS

This work was supported, in part, by the U.S. National Institutes of Health (NIH) National Institute of Mental Health Grant R01 MH094755, NIH Grant P01 AT003961, and NIH National Institute of General Medical Sciences Grant P20 GM103641 (to P.S.N.); NIH National Institute of Environmental Health Sciences Grant R01 ES019313 (to P.S.N. and M.N.); and NIH Grant R01 AT006888 and the Veterans Administration Merit Award BX001357 (to M.N.).

DISCLOSURES

The authors declare no conflict of interest.

REFERENCES

1. Wesolowski, R., Markowitz, J., Carson 3rd, W. E. (2013) Myeloid derived suppressor cells—a new therapeutic target in the treatment of cancer. *J. Immunother. Cancer* **1,** 10.
2. Keskinov, A. A., Shurin, M. R. (2015) Myeloid regulatory cells in tumor spreading and metastasis. *Immunobiology* **220,** 236–242.
3. Ugel, S., Delpozzo, F., Desantis, G., Papalini, F., Simonato, F., Sonda, N., Zilio, S., Bronte, V. (2009) Therapeutic targeting of myeloid-derived suppressor cells. *Curr. Opin. Pharmacol.* **9,** 470–481.
4. Yin, B., Ma, G., Yen, C. Y., Zhou, Z., Wang, G. X., Divino, C. M., Casares, S., Chen, S. H., Yang, W. C., Pan, P. Y. (2010) Myeloid-derived suppressor cells prevent type 1 diabetes in murine models. *J. Immunol.* **185,** 5828–5834.
5. Cripps, J. G., Gorham, J. D. (2011) MDSC in autoimmunity. *Int. Immunopharmacol.* **11,** 789–793.
6. Guan, H., Singh, N. P., Singh, U. P., Nagarkatti, P. S., Nagarkatti, M. (2012) Resveratrol prevents endothelial cells injury in high-dose interleukin-2 therapy against melanoma. *PLoS ONE* **7,** e35650.
7. Hestdal, K., Ruscetti, F. W., Ihle, J. N., Jacobsen, S. E., Dubois, C. M., Kopp, W. C., Longo, D. L., Keller, J. R. (1991) Characterization and regulation of RB6-8C5 antigen expression on murine bone marrow cells. *J. Immunol.* **147,** 22–28.
8. Movahedi, K., Guilliams, M., Van den Bossche, J., Van den Bergh, R., Gysemans, C., Beschin, A., De Baetselier, P., Van Ginderachter, J. A. (2008) Identification of discrete tumor-induced myeloid-derived suppressor cell subpopulations with distinct T cell-suppressive activity. *Blood* **111,** 4233–4244.
9. Dugast, A. S., Haudebourg, T., Coulon, F., Heslan, M., Haspot, F., Poirier, N., Vuillefroy de Silly, R., Usal, C., Smit, H., Martinet, B., Thebault, P., Renaudin, K., Vanhove, B. (2008) Myeloid-derived suppressor cells accumulate in kidney allograft tolerance and specifically suppress effector T cell expansion. *J. Immunol.* **180,** 7898–7906.
10. Nagaraj, S., Gabrilovich, D. I. (2012) Regulation of suppressive function of myeloid-derived suppressor cells by CD4+ T cells. *Semin. Cancer Biol.* **22,** 282–288.
11. Robertson, K. D. (2005) DNA methylation and human disease. *Nat. Rev. Genet.* **6,** 597–610.
12. Jeltsch, A. (2006) Molecular enzymology of mammalian DNA methyltransferases. *Curr. Top. Microbiol. Immunol.* **301,** 203–225.
13. Feinberg, A. P., Gehrke, C. W., Kuo, K. C., Ehrlich, M. (1988) Reduced genomic 5-methylcytosine content in human colonic neoplasia. *Cancer Res.* **48,** 1159–1161.
14. Baylin, S. B., Herman, J. G. (2000) DNA hypermethylation in tumorigenesis: epigenetics joins genetics. *Trends Genet.* **16,** 168–174.
15. Hamerman, J. A., Page, S. T., Pullen, A. M. (1997) Distinct methylation states of the CD8 beta gene in peripheral T cells and intraepithelial lymphocytes. *J. Immunol.* **159,** 1240–1246.
16. Fitzpatrick, D. R., Shirley, K. M., McDonald, L. E., Bielefeldt-Ohmann, H., Kay, G. F., Kelso, A. (1998) Distinct methylation of the interferon gamma (IFN-gamma) and interleukin 3 (IL-3) genes in newly activated primary CD8+ T lymphocytes: regional IFN-gamma promoter demethylation and mRNA expression are heritable in CD44(high)CD8+ T cells. *J. Exp. Med.* **188,** 103–117.
17. Cedar, H., Bergman, Y. (1999) Developmental regulation of immune system gene rearrangement. *Curr. Opin. Immunol.* **11,** 64–69.
18. Young, H. A., Ghosh, P., Ye, J., Lederer, J., Lichtman, A., Gerard, J. R., Penix, L., Wilson, C. B., Melvin, A. J., McGurn, M. E., Lewis, D. B., Taub, D. (1994) Differentiation of the T helper phenotypes by analysis of the methylation state of the IFN-gamma gene. *J. Immunol.* **153,** 3603–3610.
19. Gamper, C. J., Agoston, A. T., Nelson, W. G., Powell, J. D. (2009) Identification of DNA methyltransferase 3a as a T cell receptor-induced regulator of Th1 and Th2 differentiation. *J. Immunol.* **183,** 2267–2276.
20. Guan, H., Nagarkatti, P. S., Nagarkatti, M. (2011) CD44 reciprocally regulates the differentiation of encephalitogenic Th1/Th17 and Th2/regulatory T cells through epigenetic modulation involving DNA methylation of cytokine gene promoters, thereby controlling the development of experimental autoimmune encephalomyelitis. *J. Immunol.* **186,** 6955–6964.
21. Singh, N. P., Singh, U. P., Singh, B., Price, R. L., Nagarkatti, M., Nagarkatti, P. S. (2011) Activation of aryl hydrocarbon receptor (AhR) leads to reciprocal epigenetic regulation of FoxP3 and IL-17 expression and amelioration of experimental colitis. *PLoS ONE* **6,** e23522.
22. Chuchawankul, S., Shima, M., Buckley, N. E., Hartmann, C. B., McCoy, K. L. (2004) Role of cannabinoid receptors in inhibiting macrophage costimulatory activity. *Int. Immunopharmacol.* **4,** 265–278.
23. Sahakian, E., Powers, J. J., Chen, J., Deng, S. L., Cheng, F., Distler, A., Woods, D. M., Rock-Klotz, J., Sodre, A. L., Youn, J. I., Woan, K. V., Villagra, A., Gabrilovich, D., Sotomayor, E. M., Pinilla-Ibarz, J. (2015) Histone deacetylase 11: a novel epigenetic regulator of myeloid derived suppressor cell expansion and function. *Mol. Immunol.* **63,** 579–585.
24. Hegde, V. L., Hegde, S., Cravatt, B. F., Hofseth, L. J., Nagarkatti, M., Nagarkatti, P. S. (2008) Attenuation of experimental autoimmune hepatitis by exogenous and endogenous cannabinoids: involvement of regulatory T cells. *Mol. Pharmacol.* **74,** 20–33.
25. Nagarkatti, P., Pandey, R., Rieder, S. A., Hegde, V. L., Nagarkatti, M. (2009) Cannabinoids as novel anti-inflammatory drugs. *Future Med. Chem.* **1,** 1333–1349.

26. Pandey, R., Hegde, V. L., Nagarkatti, M., Nagarkatti, P. S. (2011) Targeting cannabinoid receptors as a novel approach in the treatment of graft-versus-host disease: evidence from an experimental murine model. *J. Pharmacol. Exp. Ther.* **338,** 819–828.
27. Klein, T. W., Friedman, H., Specter, S. (1998) Marijuana, immunity and infection. *J. Neuroimmunol.* **83,** 102–115.
28. McKallip, R. J., Nagarkatti, M., Nagarkatti, P. S. (2005) Delta-9-tetrahydrocannabinol enhances breast cancer growth and metastasis by suppression of the antitumor immune response. *J. Immunol.* **174,** 3281–3289.
29. Zhu, L. X., Sharma, S., Stolina, M., Gardner, B., Roth, M. D., Tashkin, D. P., Dubinett, S. M. (2000) Delta-9-tetrahydrocannabinol inhibits antitumor immunity by a CB2 receptor-mediated, cytokine-dependent pathway. *J. Immunol.* **165,** 373–380.
30. Hegde, V. L., Nagarkatti, M., Nagarkatti, P. S. (2010) Cannabinoid receptor activation leads to massive mobilization of myeloid-derived suppressor cells with potent immunosuppressive properties. *Eur. J. Immunol.* **40,** 3358–3371.
31. Hegde, V. L., Tomar, S., Jackson, A., Rao, R., Yang, X., Singh, U. P., Singh, N. P., Nagarkatti, P. S., Nagarkatti, M. (2013) Distinct microRNA expression profile and targeted biological pathways in functional myeloid-derived suppressor cells induced by Δ9-tetrahydrocannabinol in vivo: regulation of CCAAT/enhancer-binding protein α by microRNA-690. *J. Biol. Chem.* **288,** 36810–36826.
32. Jackson, A. R., Hegde, V. L., Nagarkatti, P. S., Nagarkatti, M. (2014) Characterization of endocannabinoid-mediated induction of myeloid-derived suppressor cells involving mast cells and MCP-1. *J. Leukoc. Biol.* **95,** 609–619.
33. Guan, H., Nagarkatti, P. S., Nagarkatti, M. (2009) Role of CD44 in the differentiation of Th1 and Th2 cells: CD44-deficiency enhances the development of Th2 effectors in response to sheep RBC and chicken ovalbumin. *J. Immunol.* **183,** 172–180.
34. Langmead, B., Trapnell, C., Pop, M., Salzberg, S. L. (2009) Ultrafast and memory-efficient alignment of short DNA sequences to the human genome. *Genome Biol.* **10,** R25.
35. Lienhard, M., Grimm, C., Morkel, M., Herwig, R., Chavez, L. (2014) MEDIPS: genome-wide differential coverage analysis of sequencing data derived from DNA enrichment experiments. *Bioinformatics* **30,** 284–286.
36. Shin, H., Liu, T., Manrai, A. K., Liu, X. S. (2009) CEAS: cis-regulatory element annotation system. *Bioinformatics* **25,** 2605–2606.
37. Rouse, M., Rao, R., Nagarkatti, M., Nagarkatti, P. S. (2014) 3,3′-Diindolylmethane ameliorates experimental autoimmune encephalomyelitis by promoting cell cycle arrest and apoptosis in activated T cells through microRNA signaling pathways. *J. Pharmacol. Exp. Ther.* **350,** 341–352.
38. Schneider, C. A., Rasband, W. S., Eliceiri, K. W. (2012) NIH Image to ImageJ: 25 years of image analysis. *Nature Methods,* **9,** 671–675.
39. Dietlin, T. A., Hofman, F. M., Lund, B. T., Gilmore, W., Stohlman, S. A., van der Veen, R. C. (2007) Mycobacteria-induced Gr-1+ subsets from distinct myeloid lineages have opposite effects on T cell expansion. *J. Leukoc. Biol.* **81,** 1205–1212.
40. Zhu, B., Bando, Y., Xiao, S., Yang, K., Anderson, A. C., Kuchroo, V. K., Khoury, S. J. (2007) CD11b+Ly-6C(hi) suppressive monocytes in experimental autoimmune encephalomyelitis. *J. Immunol.* **179,** 5228–5237.
41. Kusmartsev, S., Gabrilovich, D. I. (2005) STAT1 signaling regulates tumor-associated macrophage-mediated T cell deletion. *J. Immunol.* **174,** 4880–4891.
42. Sinha, P., Okoro, C., Foell, D., Freeze, H. H., Ostrand-Rosenberg, S., Srikrishna, G. (2008) Proinflammatory S100 proteins regulate the accumulation of myeloid-derived suppressor cells. *J. Immunol.* **181,** 4666–4675.
43. Trikha, P., Carson III, W. E. (2014) Signaling pathways involved in MDSC regulation. *Biochim. Biophys. Acta* **1846,** 55–65.
44. Wu, L., Du, H., Li, Y., Qu, P., Yan, C. (2011) Signal transducer and activator of transcription 3 (Stat3C) promotes myeloid-derived suppressor cell expansion and immune suppression during lung tumorigenesis. *Am. J. Pathol.* **179,** 2131–2141.
45. Lozovan, M. G., Pichugina, L. A., Nikitenko, L. D., Bobrik, L. M., Stratanovich, M. G. (1990) [Association of Wegener's granulomatosis and tumor process]. *Probl. Tuberk.* 73–75.
46. Vasquez-Dunddel, D., Pan, F., Zeng, Q., Gorbounov, M., Albesiano, E., Fu, J., Blosser, R. L., Tam, A. J., Bruno, T., Zhang, H., Pardoll, D., Kim, Y. (2013) STAT3 regulates arginase-I in myeloid-derived suppressor cells from cancer patients. *J. Clin. Invest.* **123,** 1580–1589.
47. Cheng, P., Corzo, C. A., Luetteke, N., Yu, B., Nagaraj, S., Bui, M. M., Ortiz, M., Nacken, W., Sorg, C., Vogl, T., Roth, J., Gabrilovich, D. I. (2008) Inhibition of dendritic cell differentiation and accumulation of myeloid-derived suppressor cells in cancer is regulated by S100A9 protein. *J. Exp. Med.* **205,** 2235–2249.
48. Compton, D. R., Gold, L. H., Ward, S. J., Balster, R. L., Martin, B. R. (1992) Aminoalkylindole analogs: cannabimimetic activity of a class of compounds structurally distinct from delta 9-tetrahydrocannabinol. *J. Pharmacol. Exp. Ther.* **263,** 1118–1126.
49. Okano, M., Xie, S., Li, E. (1998) Cloning and characterization of a family of novel mammalian DNA (cytosine-5) methyltransferases. *Nat. Genet.* **19,** 219–220.
50. McKallip, R. J., Lombard, C., Martin, B. R., Nagarkatti, M., Nagarkatti, P. S. (2002) Delta(9)-tetrahydrocannabinol-induced apoptosis in the thymus and spleen as a mechanism of immunosuppression in vitro and in vivo. *J. Pharmacol. Exp. Ther.* **302,** 451–465.
51. Hoechst, B., Gamrekelashvili, J., Manns, M. P., Greten, T. F., Korangy, F. (2011) Plasticity of human Th17 cells and iTregs is orchestrated by different subsets of myeloid cells. *Blood* **117,** 6532–6541.
52. Peláez, B., Campillo, J. A., López-Asenjo, J. A., Subiza, J. L. (2001) Cyclophosphamide induces the development of early myeloid cells suppressing tumor cell growth by a nitric oxide-dependent mechanism. *J. Immunol.* **166,** 6608–6615.
53. Yang, X., Hegde, V. L., Rao, R., Zhang, J., Nagarkatti, P. S., Nagarkatti, M. (2014) Histone modifications are associated with Delta(9)-tetrahydrocannabinol-mediated alterations in antigen-specific T cell responses. *J. Biol. Chem.* **289,** 18707–18718.
54. Bonnin, A., de Miguel, R., Hernández, M. L., Ramos, J. A., Fernández-Ruiz, J. J. (1995) The prenatal exposure to delta 9-tetrahydrocannabinol affects the gene expression and the activity of tyrosine hydroxylase during early brain development. *Life Sci.* **56,** 2177–2184.
55. Hernández, M. L., García-Gil, L., Berrendero, F., Ramos, J. A., Fernández-Ruiz, J. J. (1997) Delta 9-tetrahydrocannabinol increases activity of tyrosine hydroxylase in cultured fetal mesencephalic neurons. *J. Mol. Neurosci.* **8,** 83–91.
56. Pérez-Rosado, A., Manzanares, J., Fernández-Ruiz, J., Ramos, J. A. (2000) Prenatal Delta(9)-tetrahydrocannabinol exposure modifies proenkephalin gene expression in the fetal rat brain: sex-dependent differences. *Brain Res. Dev. Brain Res.* **120,** 77–81.
57. Gómez, M., Hernández, M., Johansson, B., de Miguel, R., Ramos, J. A., Fernández-Ruiz, J. (2003) Prenatal cannabinoid and gene expression for neural adhesion molecule L1 in the fetal rat brain. *Brain Res. Dev. Brain Res.* **147,** 201–207.
58. Maccarrone, M., Finazzi-Agró, A. (2003) The endocannabinoid system, anandamide and the regulation of mammalian cell apoptosis. *Cell Death Differ.* **10,** 946–955.
59. Molina, P. E., Amedee, A., LeCapitaine, N. J., Zabaleta, J., Mohan, M., Winsauer, P., Vande Stouwe, C. (2011) Cannabinoid neuroimmune modulation of SIV disease. *J. Neuroimmune Pharmacol.* **6,** 516–527.
60. Paradisi, A., Pasquariello, N., Barcaroli, D., Maccarrone, M. (2008) Anandamide regulates keratinocyte differentiation by inducing DNA methylation in a CB1 receptor-dependent manner. *J. Biol. Chem.* **283,** 6005–6012.
61. Nelson, E. D., Kavalali, E. T., Monteggia, L. M. (2008) Activity-dependent suppression of miniature neurotransmission through the regulation of DNA methylation. *J. Neurosci.* **28,** 395–406.
62. Delano, M. J., Scumpia, P. O., Weinstein, J. S., Coco, D., Nagaraj, S., Kelly-Scumpia, K. M., O'Malley, K. A., Wynn, J. L., Antonenko, S., Al-Quran, S. Z., Swan, R., Chung, C. S., Atkinson, M. A., Ramphal, R., Gabrilovich, D. I., Reeves, W. H., Ayala, A., Phillips, J., Laface, D., Heyworth, P. G., Clare-Salzler, M., Moldawer, L. L. (2007) MyD88-dependent expansion of an immature GR-1(+)CD11b(+) population induces T cell suppression and Th2 polarization in sepsis. *J. Exp. Med.* **204,** 1463–1474.
63. Lee, I. T., Lin, C. C., Wang, C. H., Cherng, W. J., Wang, J. S., Yang, C. M. (2013) ATP stimulates PGE(2)/cyclin D1-dependent VSMCs proliferation via STAT3 activation: role of PKCs-dependent NADPH oxidase/ROS generation. *Biochem. Pharmacol.* **85,** 954–964.
64. Hegde, V. L., Nagarkatti, P. S., Nagarkatti, M. (2011) Role of myeloid-derived suppressor cells in amelioration of experimental autoimmune hepatitis following activation of TRPV1 receptors by cannabidiol. *PLoS ONE* **6,** e18281.
65. Rodriguez, P. C., Quiceno, D. G., Ochoa, A. C. (2007) L-Arginine availability regulates T-lymphocyte cell-cycle progression. *Blood* **109,** 1568–1573.
66. Kusmartsev, S., Nefedova, Y., Yoder, D., Gabrilovich, D. I. (2004) Antigen-specific inhibition of CD8+ T cell response by immature myeloid cells in cancer is mediated by reactive oxygen species. *J. Immunol.* **172,** 989–999.
67. Pan, P. Y., Ma, G., Weber, K. J., Ozao-Choy, J., Wang, G., Yin, B., Divino, C. M., Chen, S. H. (2010) Immune stimulatory receptor CD40 is required for T-cell suppression and T regulatory cell activation mediated by myeloid-derived suppressor cells in cancer. *Cancer Res.* **70,** 99–108.
68. Srivastava, M. K., Sinha, P., Clements, V. K., Rodriguez, P., Ostrand-Rosenberg, S. (2010) Myeloid-derived suppressor cells inhibit T-cell activation by depleting cystine and cysteine. *Cancer Res.* **70,** 68–77.

69. Howlett, A. C., Blume, L. C., Dalton, G. D. (2010) CB(1) cannabinoid receptors and their associated proteins. *Curr. Med. Chem.* **17,** 1382–1393.
70. Jeon, Y. J., Yang, K. H., Pulaski, J. T., Kaminski, N. E. (1996) Attenuation of inducible nitric oxide synthase gene expression by delta 9-tetrahydrocannabinol is mediated through the inhibition of nuclear factor- kappa B/Rel activation. *Mol. Pharmacol.* **50,** 334–341.
71. Ichikawa, M., Williams, R., Wang, L., Vogl, T., Srikrishna, G. (2011) S100A8/A9 activate key genes and pathways in colon tumor progression. *Mol. Cancer Res.* **9,** 133–148.
72. Hiroshima, Y., Hsu, K., Tedla, N., Chung, Y. M., Chow, S., Herbert, C., Geczy, C. L. (2014) S100A8 induces IL-10 and protects against acute lung injury. *J. Immunol.* **192,** 2800–2811.
73. Simard, J. C., Cesaro, A., Chapeton-Montes, J., Tardif, M., Antoine, F., Girard, D., Tessier, P. A. (2013) S100A8 and S100A9 induce cytokine expression and regulate the NLRP3 inflammasome via ROS-dependent activation of NF-κB(1.). *PLoS ONE* **8,** e72138.
74. Goyette, J., Geczy, C. L. (2011) Inflammation-associated S100 proteins: new mechanisms that regulate function. *Amino Acids* **41,** 821–842.
75. Munder, M., Eichmann, K., Morán, J. M., Centeno, F., Soler, G., Modolell, M. (1999) Th1/Th2-regulated expression of arginase isoforms in murine macrophages and dendritic cells. *J. Immunol.* **163,** 3771–3777.
76. El Kasmi, K. C., Qualls, J. E., Pesce, J. T., Smith, A. M., Thompson, R. W., Henao-Tamayo, M., Basaraba, R. J., König, T., Schleicher, U., Koo, M. S., Kaplan, G., Fitzgerald, K. A., Tuomanen, E. I., Orme, I. M., Kanneganti, T. D., Bogdan, C., Wynn, T. A., Murray, P. J. (2008) Toll-like receptor-induced arginase 1 in macrophages thwarts effective immunity against intracellular pathogens. *Nat. Immunol.* **9,** 1399–1406.
77. Vogl, T., Tenbrock, K., Ludwig, S., Leukert, N., Ehrhardt, C., van Zoelen, M. A., Nacken, W., Foell, D., van der Poll, T., Sorg, C., Roth, J. (2007) Mrp8 and Mrp14 are endogenous activators of Toll-like receptor 4, promoting lethal, endotoxin-induced shock. *Nat. Med.* **13,** 1042–1049.
78. van Lent, P. L., Grevers, L. C., Schelbergen, R., Blom, A., Geurts, J., Sloetjes, A., Vogl, T., Roth, J., van den Berg, W. B. (2010) S100A8 causes a shift toward expression of activatory Fcγ receptors on macrophages via toll-like receptor 4 and regulates Fcγ receptor expression in synovium during chronic experimental arthritis. *Arthritis Rheum.* **62,** 3353–3364.
79. Klempt, M., Melkonyan, H., Hofmann, H. A., Eue, I., Sorg, C. (1998) The transcription factors c-myb and C/EBP alpha regulate the monocytic/myeloic gene MRP14. *Immunobiology* **199,** 148–151.
80. Rao, R., Nagarkatti, P. S., Nagarkatti, M. (2014) Δ(9) Tetrahydrocannabinol attenuates *Staphylococcal enterotoxin* B-induced inflammatory lung injury and prevents mortality in mice by modulation of miR-17-92 cluster and induction of T-regulatory cells. *Br. J. Pharmacol.* doi: 10.1111/bph.13026 [Epub ahead of print].

KEY WORDS:
DNA methylation · T cell suppression · arginase 1 · cannabinoid